Earth Planets Space, **61**, 525–533, 2009

Temporal and spatial distributions of atmospheric wave energy in the equatorial stratosphere revealed by GPS radio occultation temperature data obtained with the CHAMP satellite during 2001–2006

Toshitaka Tsuda[1], M. Venkat Ratnam[1,2], Simon P. Alexander[1], Toshiaki Kozu[3], and Yukari Takayabu[4]

[1]*Research Institute for Sustainable Humanosphere (RISH), Kyoto University, Japan*
[2]*National Atmospheric Research Laboratory (NARL), Gadanki, India*
[3]*Faculty of Science and Engineering, Shimane University, Japan*
[4]*Center for Climate System Research (CCSR), University of Tokyo, Japan*

(Received January 30, 2008; Revised April 25, 2008; Accepted May 15, 2008; Online published May 14, 2009)

Using stratospheric temperature profiles derived from GPS radio occultation (RO) measurements made by the German CHAMP satellite from June 2001 to May 2006, we studied the climatological behavior of atmospheric wave activity in the tropics. The wave potential energy, E_p, is calculated from temperature fluctuations with vertical scales shorter than 7 km in a longitude and latitude cell of $20^\circ \times 10^\circ$ at 19–26 km. E_p is then averaged every 3 months (June–July–August (JJA), September–October–November (SON), December–January–February (DJF), March–April–May (MAM)), and the averages are compared with the cloud top temperature from outgoing long-wave radiation (OLR) and the convective rain rate from the TRMM precipitation radar (PR). E_p at 19–26 km in the western Pacific to Indian Ocean is found to show a clear seasonal variation, with a large E_p during DJF and MAM and a considerably enhanced E_p in SON; it becomes minimum during JJA near the equator, when the center of the enhanced E_p region appears over north India and the Indochina peninsula. Localized enhancement of E_p seems to be mainly due to atmospheric gravity waves. In addition, the longitudinally elongated portion of E_p is partially affected by Kelvin wave-like disturbances with short horizontal scales. In DJF and MAM, the convective clouds are located over the western Pacific and around Indonesia, at which time the Kelvin wave-like disturbances are effectively generated. The spatial and seasonal variations of E_p are closely related to the distribution of clouds, implying that convective wave generation is very important in the tropics. However, wave-mean flow interactions due to the wind shear of the QBO become important in the lower stratosphere, which considerably modifies our analysis of the E_p distribution at 19–26 km. Therefore, both wave generation and propagation characteristics must be taken into account in describing the climatological behavior of atmospheric wave activity in the equatorial stratosphere.

Key words: Gravity wave, Kelvin wave, equatorial atmosphere, GPS occultation.

1. Introduction

Active convection in the tropics generates various waves, such as Kelvin waves, tides, gravity waves, among others. Wave energy and momentum are transported upward by these vertically propagating waves (e.g., Fritts and Alexander, 2003). A knowledge of wave-mean flow interactions are crucially important for understanding dynamical processes in the equatorial atmosphere, including the formation of peculiar long-term variations such as the quasi-biennial oscillation (QBO) and the semi-annual oscillation (SAO) in the stratosphere and the mesosphere and lower thermosphere (MLT) region (70–150 km).

In order to clarify the behavior of atmospheric waves in the equatorial region in general and that over the Indonesian maritime-continent in particular, a number of intensive campaigns with balloon-borne radiosondes have been conducted (e.g., Tsuda *et al*., 1994, 2006). However, the horizontal distribution of wave energy in the equatorial stratosphere can not be fully clarified using ground-based measurements because of the sparse distribution of observation stations for routine radiosonde soundings, wind profiling radars, and other measurement tools.

The global distribution of stratospheric wave activity has also been studied by employing a novel GPS radio occultation (RO) technique (Tsuda *et al*., 2000; Ratnam *et al*., 2004). The GPS signals received on low Earth orbiting (LEO) satellites are then used for active limb-sounding of the atmosphere. Recent GPS RO missions, such as the Challenging Mini-Payload (CHAMP) satellite and the Constellation Observing System for Meteorology, Ionosphere and Climate (COSMIC) missions, have achieved significant progress in measuring accurate temperature profiles below 35–40 km. The GPS RO data are characterized by a good height resolution, comparable to radiosondes, and they are particularly valuable in the tropics where routine radiosonde observations are sparse.

The long-term behavior of temperature variance was studied by using CHAMP GPS RO data during a 5-year period from May 2001 to April 2006 (de la Torre *et al.*, 2006). These researchers reported the latitude, height, and time variations of stratospheric wave activity with vertical wave lengths shorter than 10 km, but they did not discuss any horizontal variations, as the variance was averaged zonally. At equatorial latitudes, the stratospheric wave activity generally showed an annual variation, but it was largely affected by the QBO as the wave energy was enhanced just below zonal wind contours, corresponding to eastward shear. This feature had already been studied by Randel and Wu (2005) in their analysis of CHAMP GPS RO data.

Using CHAMP GPS RO data for 2001–2006, we studied the climatological behavior of the horizontal distribution of atmospheric wave energy in the tropical stratosphere, and its long-term variation in relation to convective activity and background wind conditions, such as the Walker circulation and the stratospheric QBO. We also analyzed spatial and temporal variations of convective activity using outgoing long-wave radiation (OLR) data and rainfall data from the precipitation radar (PR) on-board the Tropical Rainfall Measuring Mission (TRMM) satellite. We used routine radiosonde data collected by the Malaysian Meteorological Department to study the interaction between gravity waves and the stratospheric QBO.

2. Data Analysis

The German CHAMP satellite was launched in July 2000 on a near-polar (inclination: 87°) orbit. The GPS RO with CHAMP provides temperature profiles up to 35 km. In our study, we use level-3 version 005 GPS RO data processed at Geo Forschungs Zentrum (GFZ), Potsdam (Wickert *et al.*, 2001). GFZ provides about 2,000–4,500 profiles globally every month. The vertical resolution of the temperature profiles ranges from 0.5 km in the lower troposphere to 1.4 km in the stratosphere, and the horizontal resolution along the GPS ray path is about a few hundred kilometers. Therefore, the GPS RO temperature profiles are not sensitive to gravity waves with short horizontal wavelengths.

We use the CHAMP temperature data for a 5-year period (June 2001 to May 2006). We analyze the potential energy of atmospheric waves using a similar method to that of Hei *et al.* (2008), which is briefly summarized below. The wave potential energy E_p that is used as the measure of wave activity is defined as follows:

$$E_p = \frac{1}{2}\left(\frac{g}{N}\right)^2\left(\frac{T'}{T_0}\right)^2 \quad (1)$$

where T' is the temperature fluctuation, T_0 is the background temperature, N is the Brunt-Väisälä frequency, and g is the gravitational acceleration.

We accumulate all available temperature profiles in 1 month in a cell of 20° × 10° in longitude and latitude, then low-pass filter them using a 4-km vertical running mean. This is defined as T_0 in each cell. We obtain T' by subtracting T_0 from individual GPS RO profiles. We apply the Fast Fourier Transform (FFT) at 12–33 km and extract T' with vertical wave lengths shorter than 7 km. E_p is then determined from individual profiles at 12–19 km, 19–26 km, and 26–33 km, which are then averaged in each cell for each month. Note that the E_p values at 12–19 km in the tropics could be contaminated by spurious temperature perturbations due to the sharp temperature gradient changes around the tropopause at 15–17 km. Therefore, we use the results at 19–26 km in our study. Note that de la Tore *et al.* (2006) also set the minimum altitude for the wave variance analysis at 19 km, after considering the effects of the sharp tropical tropopause. Taking into account the filter bandwidths for the vertical and horizontal wavelength, we assume that the analyzed E_p consists of gravity waves, equatorially trapped Kelvin waves with horizontal wave numbers of 1 to 9, and a part of mixed Rossby gravity waves. However, despite the inclusion of some equatorially trapped Kelvin waves in the analysis, the major contribution to E_p seems to be small-scale gravity waves (Randel and Wu, 2005).

Although Hei *et al.* (2008) used the monthly E_p values for their study of gravity waves in the polar regions, we average the data over 3 months in order to obtain a significant number of data points in each cell because the data density of CHAMP GPS RO is the least in the tropics due to the satellite high orbit inclination angle.

In addition to the GPS RO data, we use satellite rainfall data with TRMM-PR and OLR as a proxy for tropical convection. TRMM was launched in 1997 and carries a radar operating at 13.8 GHz for observing rainfall (precipitation radar; PR) (Kozu *et al.*, 2001). TRMM-PR provides precipitation data in the tropics equatorward of 36°, and it takes about 46 days to make enough measurements with a homogenous data distribution in local time to reduce the sampling bias due to the diurnal cycle of precipitation. We use the 3A25 version 6 data product in this study, and the data are averaged over 3 months, corresponding to the GPS RO results, in a longitude-latitude cell of 5° × 5°. OLR data provided by National Oceanic and Atmospheric Administration (NOAA) are available at a 2.5° × 2.5° longitude-latitude grid and also averaged every 3 months.

We also use routine radiosonde data from Kuala Lumpur (2.73°N, 101.70°E) during 2004–2005, which are specially analyzed by the Malaysian Meteorological Department to have a height resolution of about 100 m.

3. Results

3.1 Comparison between E_p and cloud distributions

Figure 1 shows the horizontal distribution of E_p averaged for 3 months in June–July–August (JJA) 2001, September–October–November (SON) 2001, and December–January–February (DJF) 2001/2002 in comparison with cloud distribution, with the distribution of cloud top temperature from OLR and the convective rain rate from TRMM-PR.

During JJA, precipitation due to the Asian monsoon is most active over India, the Bay of Bengal, and south-eastern Asia. Convective activity also seems to be enhanced around the Philippines. A similar distribution is evident in E_p, such that it is enhanced over the Asian monsoon region as well as the Philippines. Large E_p values are also recognized in South America and Africa, which shows an overall consistency with cloud distribution. The convective rain rate with TRMM-PR shows a better correlation with E_p than OLR, especially over Africa and the Indian Ocean. Note, how-

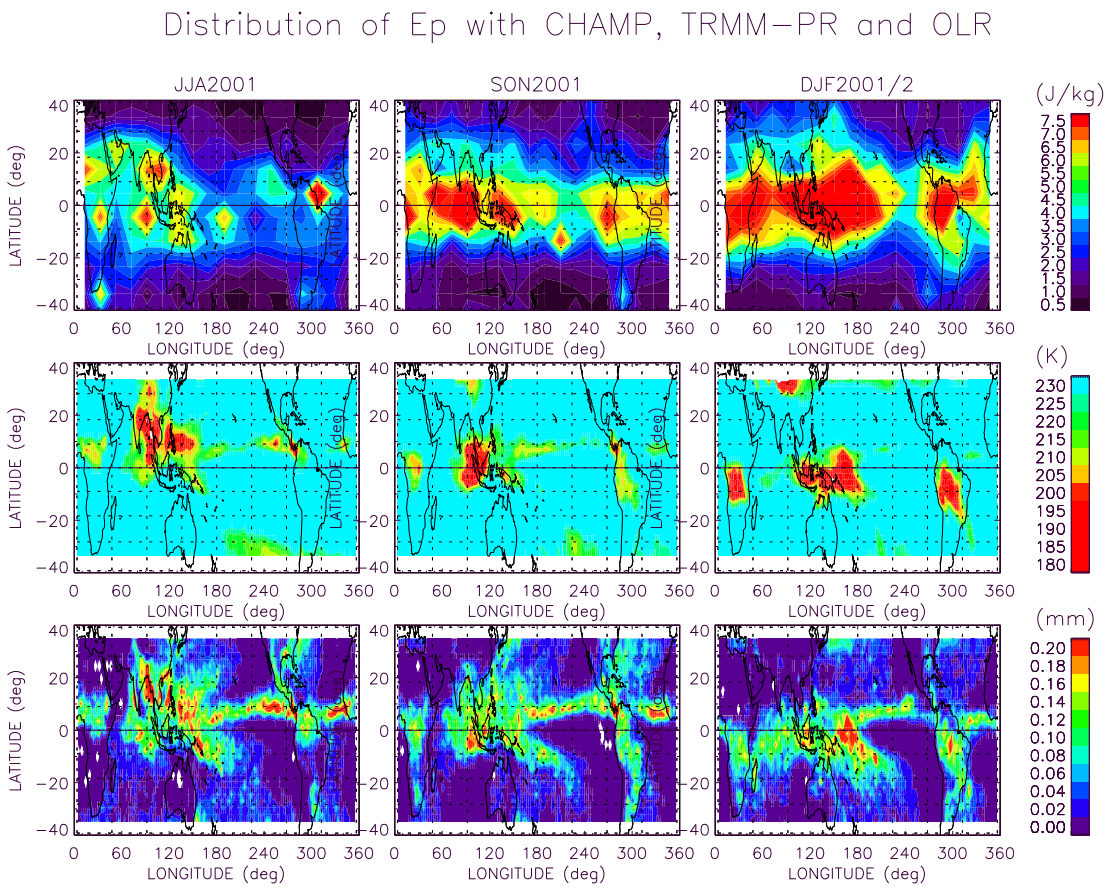

Fig. 1. Longitude-latitude distribution of E_p (top), OLR (middle), and TRMM-PR (bottom) results averaged for 3 months during (a) June–July–August 2001, (b) September–October–November 2001 and (c) December–January–February 2001/2002, respectively.

ever, that intense convection along the Intertropical Convergence Zone (ITCZ) in the eastern Pacific Ocean does not correspond to large E_p, probably because the maximum storm height at ITCZ is mostly lower than about 5 km, as determined from TRMM-PR results (not shown). Thus, the convective activity there may not be effective in generating waves that can penetrate into the stratosphere.

During SON 2001, the OLR map indicates that the center of clouds moved southward and stayed over the equatorial region, centering on Sumatra island. TRMM-PR shows a more detailed distribution of the convective rain, which was centered to the west of Sumatra. Large E_p appeared around Indonesia, whose distribution seems more consistent with the TRMM-PR results. E_p was again not enhanced over the ITCZ, but rather the distribution of E_p was elongated along longitude over the equator.

In DJF, E_p is enhanced largely over the western Pacific and Indonesia, in response to the intense convective rain in the corresponding area. Enhanced E_p regions over Africa and South America are also consistent with the OLR and TRMM-PR distributions. However, the center of E_p is still at the equator, despite these three convective regions being south of the equator. This implies that equatorially trapped Kelvin waves with a symmetric latitudinal structure seem to be effectively generated by the tropical convection. Therefore, the enhanced E_p near the equator may not be fully attributed to gravity waves, but also include Kelvin waves with vertical wavelengths shorter than 7 km (e.g., Holton *et al.*, 2001). Such phenomena may not be classified as conventional Kelvin waves with a full zonal propagation, but they should be called Kelvin wave-like disturbances, as the wave activity is not zonally symmetric but localized around the source region.

3.2 Seasonal variations of E_p in 2001–2006

Figure 2 shows the 3-month determinations of E_p at 19–26 km from June 2001 to May 2006. The seasonal variations of the E_p distribution in the western Pacific can, in general, be characterized by having its maximum in DJF and MAM; it is also considerably enhanced in SON. In JJA, E_p reaches a minimum, and its center is shifted towards the north. The distribution of E_p is typically characterized by two categories: (1) a longitudinally elongated pattern centered on the equator and (2) localized patchy ones which do not necessarily appear over the equator.

The localized E_p seems to be mainly a result of atmospheric gravity waves, as discussed in detail in Fig. 1. However, the longitudinally homogenous portion of E_p could be partially affected by Kelvin wave-like disturbances with short vertical wave lengths. Such features are evident in DJF in 2003/2004 and 2005/2006 as well as MAM in 2004 and 2006. When the convective heat source is located over the equator, as in Fig. 1(c), Kelvin-wave-like disturbances seem to be effectively generated.

A biennial cycle can clearly be recognized in Fig. 2; for example, the E_p in the western Pacific was enhanced in DJF in 2001/2002, 2003/2004, and 2005/2006, but it

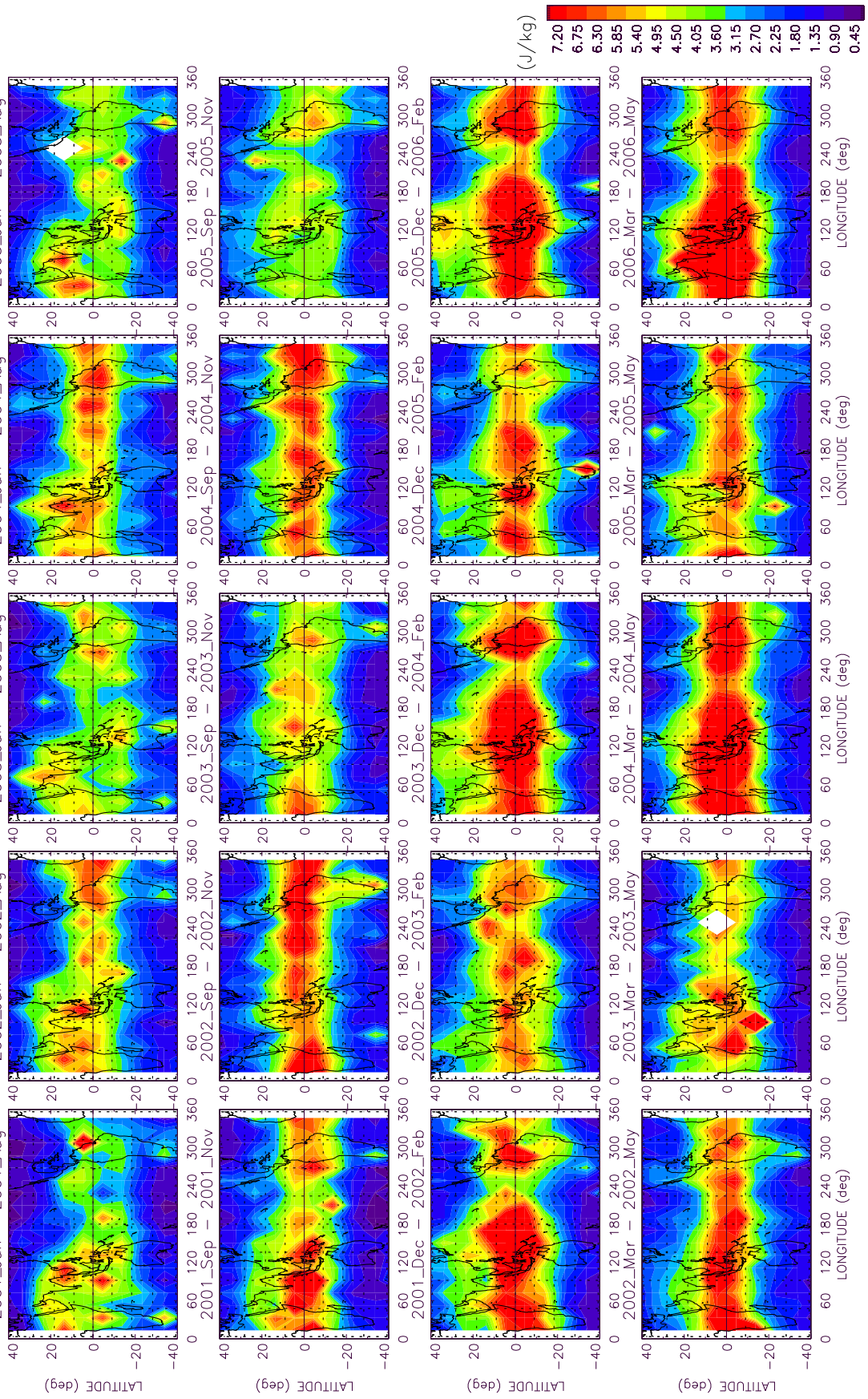

Fig. 2. The longitude-latitude distribution of E_p analyzed every 3 months from June 2001 to May 2006. From the top to bottom panels, results are plotted for June–July–August, September–October–November, December–January–February, and March–April–May, respectively.

was suppressed in 2002/2003 and 2004/2005, which seem to be a result of the wave-mean flow interaction with the QBO, as reported by de la Torre *et al.* (2006), who also used CHAMP GPS RO data. A comparable interaction was also reported by Sato and Dunkerton (1997) using routine radiosonde soundings at Singapore. Therefore, although the spatial distributions and seasonal variations of E_p are closely related with convective activity, wave propagation characteristics, such as wave-mean flow interaction, must also be taken into account when describing the temporal variations of the E_p distribution in the tropics.

3.3 Year-to-year variations of E_p during DJF

Figure 3 shows the E_p and cloud distributions in DJF during the 5 years of 2001/2002–2005/2006. (The Left-hand panels are the same as Fig. 1(c).) The bottom panel of Fig. 3 shows the longitude variations of E_p, OLR, and TRMM-PR data that are averaged in a latitude band from 10°N to 10°S. The distribution of OLR and TRMM-PR are similar in 2001/2002, 2003/2004, and 2004/2005, with an enhanced region in the western Pacific, Africa, and South America. However, in 2002/2003, the clouds in the Pacific split between the Indonesian region and the central Pacific near the date line (180°E), which seems to be caused by an El Nino event. In 2005/2006, convective activity in the western Pacific was considerably enhanced, probably due to the effects of La Nina.

In 2002/2003 and 2004/2005, when the wave-mean flow interaction prohibited the upward propagation of gravity waves into the lower stratosphere (19–26 km), the convective activity does not seem to be directly related to the stratospheric E_p. However, in other years, i.e., 2001/2002, 2003/2004, and 2005/2006, a quite interesting correlation can be recognized. In 2003/2004, the active convection region was split into the longitude sectors at around 110°E and 160°E; at this time, the peak of E_p also appeared separately at 90°E and 170°E. The longitude shift between the clouds and E_p could be attributed to horizontal propagation of atmospheric waves from the source region, but we are not sure whether this is meaningful (note that the longitude resolution of E_p is 20°). The bottom panel in Fig. 3 indicates that in 2001/2002 the cloud region was similarly separated into two at 100°E and 150°E, although its intensity was much larger for the 150°E peak; the E_p also showed two split peaks with the magnitude difference consistent with the cloud parameters. In 2005/2006, a dip in the cloud distribution is seen at around 130°E, though small, and E_p was enhanced in two longitude regions as in 2001/2002 and 2003/2004. It is likely that the E_p distributions in 2001/2002, 2003/2004, and 2005/2006 directly reflected the activity of convective activity.

Convective activity over South America was very similar between the five years. The E_p characteristics were also nearly the same in 2001/2002, 2003/2004 and 2005/2006 when the wave-mean flow interaction was not significant.

3.4 Effects of wave-mean flow interactions

Here, we investigate the interaction of gravity waves and the background mean flow using routine radiosonde profiles with a height resolution of 100 m collected four times per day at Kuala Lumpur (KL; 2.73°N, 101.70°E) in 2004–2005.

For the characterization of inertia-gravity waves (periods < 3 days), we have subtracted the monthly mean values at each altitude and then applied a high-pass filter with a cutoff at 3 days so that the effects of long-period waves (such as Kelvin waves) are removed. Taking into account that the dominant vertical wavelengths of gravity waves are about 3 km, we apply a further high-pass filter to the vertical profiles with a cut-off at 5 km. Since the time resolution of the radiosonde launch is 6 h, the filtered fluctuations consist of gravity waves with periods ranging from 12 h to 3 days.

We have estimated the kinetic energy (E_k) per unit mass of the gravity waves using the above obtained perturbations of wind velocity variance as follows:

$$E_k = \frac{1}{2}\left(u'^2 + v'^2\right) \tag{2}$$

where primes indicate the perturbation components, and the wind velocity variance is averaged over 3 days but no integration is applied along altitude. Note that the effect of vertical wind velocity—i.e., $1/2w'^2$ was not included in Eq. (2)—as its contribution is very small. The wave potential energy, E_p, is also calculated in a similar way from the radiosonde data.

Contour plots in the top and middle panels of Fig. 4 show the time-height cross-section of E_p and E_k, respectively. Superimposed contours in these panels show the zonal wind at KL (solid/dotted lines for eastward/westward components, respectively). The bottom panel of Fig. 4 shows the time-longitude distribution of the OLR deviation (sign reversed) from the yearly mean at 0–2.5°N with a cell size of $2.5° \times 2.5°$ in longitude-latitude.

Figure 4 indicates that enhanced wave activity in the lower stratosphere is clearly observed during the eastward winds of QBO (dotted line) and not seen during the westward winds (solid line). Researchers using data from radiosonde campaigns in Sumatra, Indonesia during April–May 2004 often noticed that most of waves in the stratosphere propagated eastward (Ratnam *et al.*, 2006b). Similar features were also observed during another campaign at the same site in December 2005. It is noteworthy that westward winds persistently existed at 10–15 km throughout 2004–2005 due to the Walker circulation. It is likely that both eastward and westward propagating waves can be generated in the troposphere due to convective activity but that upward propagating westward gravity wave components are removed in westward winds at 10–15 km, leaving only eastward components in the stratosphere, which further interact with the QBO.

Figure 2 shows that E_p around KL was relatively enhanced in SON in 2004 but it was much weaker in the same months in 2005. These analyses interval and height ranges are indicated by the black and red squares in the top panel of Fig. 2 for 2004 and 2005, respectively. The bottom panel in Fig. 4 suggests that convective activity in SON at KL (location indicated by a yellow line) was similar between 2004 and 2005, or even stronger in 2005. However, upward propagating waves seem to be absorbed below about 20 km in 2005 due to wave-mean flow interaction.

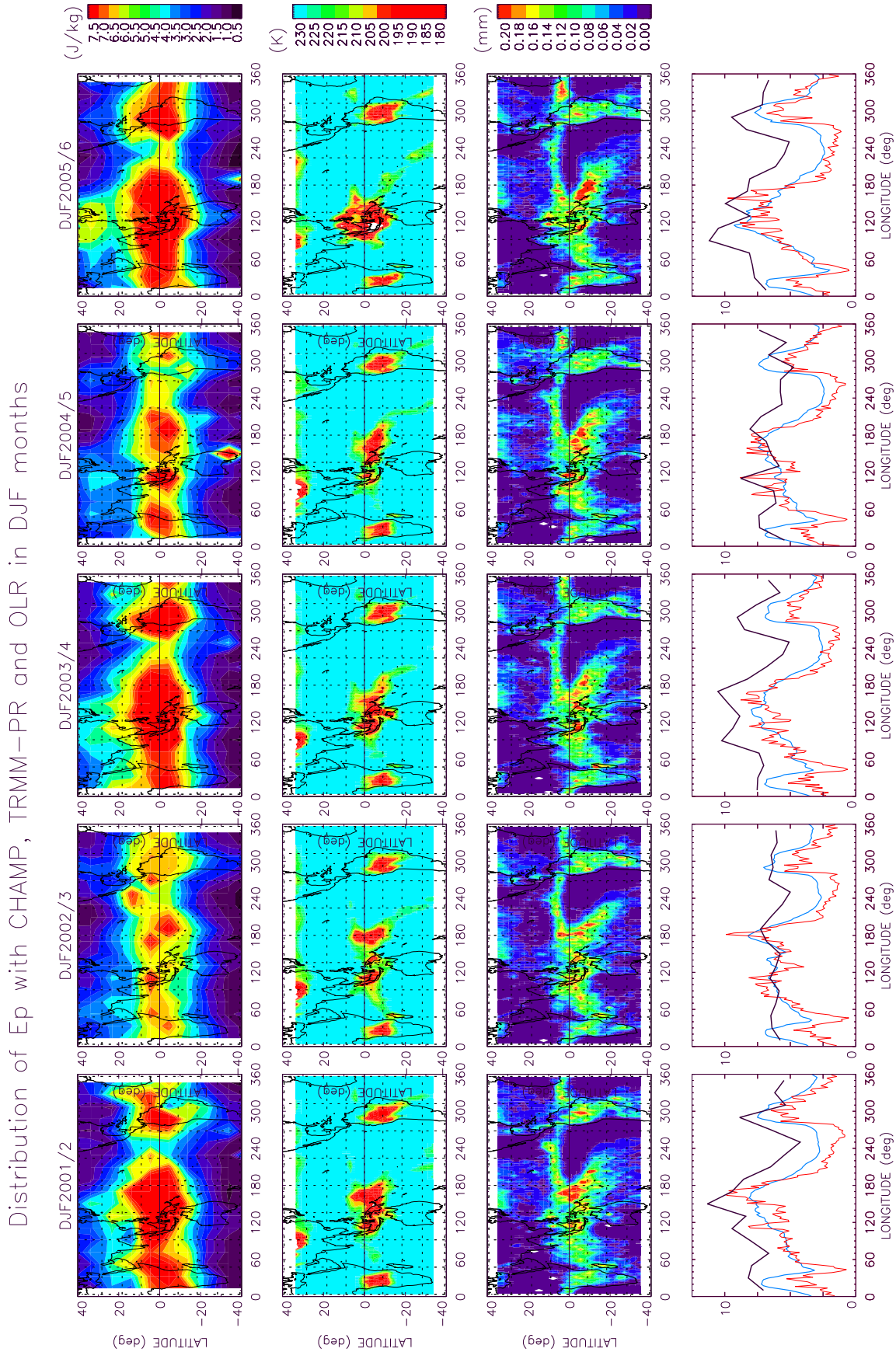

Fig. 3. E_p (top), OLR (2nd row), and TRMM-PR (3rd row) results for December–January–February during 2001/2002, 2002/2003, 2003/2004, 2004/2005, and 2005/2006 (from left to right). The longitude variations of E_p (black), OLR (blue), and convective rain rate (red) averaged between 10°N and 10°S are plotted in the bottom panel. Note that in the bottom panel the axis shows the value of E_p (in J/kg), and the range of OLR and convective rain rate corresponds to 300–150 (K) and 0–0.25 (mm), respectively.

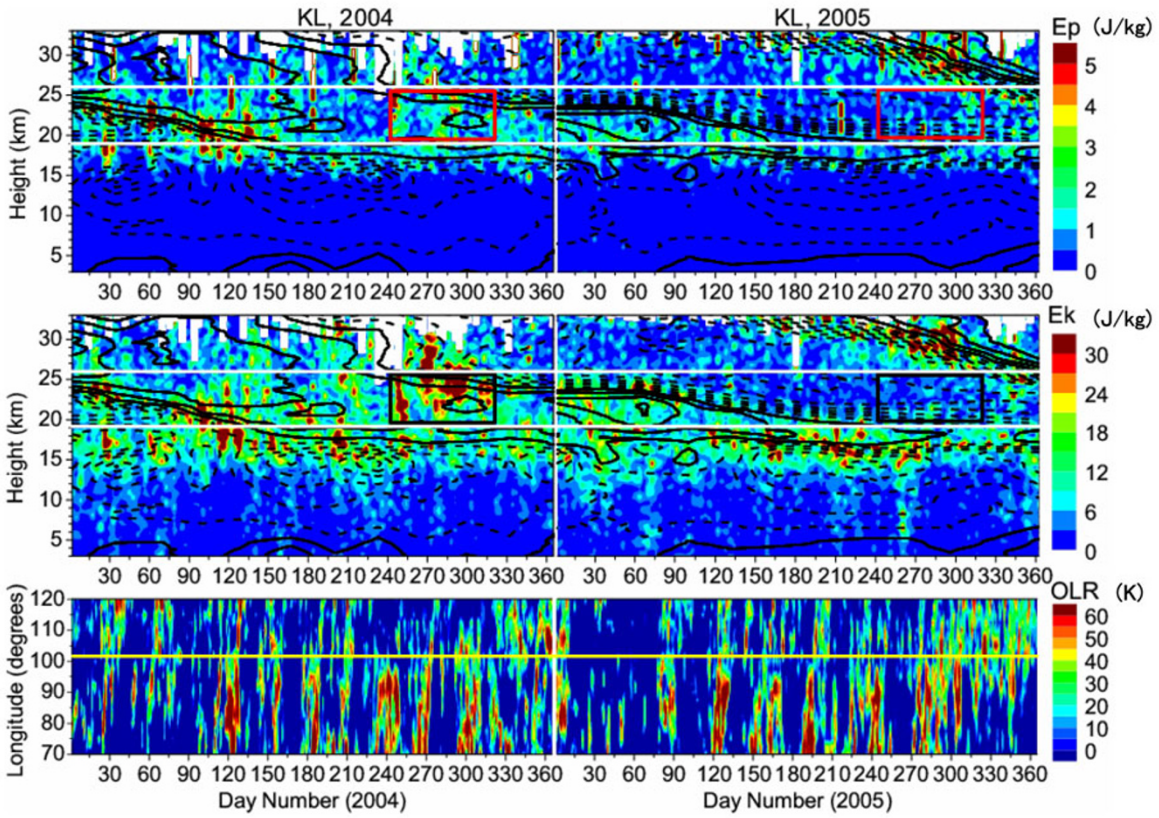

Fig. 4. Time-height section of E_p (top panel) and E_k (middle panel) analyzed from routine radiosonde observations at Kuala Lumpur in 2004–2005. Superimposed contours, plotted with an interval of 5 m/s, are the zonal winds at KL, where the solid and dotted lines correspond to the eastward and westward components, respectively. The bottom panel shows the time-longitude distribution of the OLR deviation from the yearly mean in each longitude cell. A horizontal line in the bottom panel indicates the longitude for KL.

3.5 Climatological distribution of E_p

In order to obtain climatological characteristics of the E_p distribution in the tropics, we averaged the E_p values in Fig. 2 in each season for 5 years, and plotted them in the left panels in Fig. 5. These mean E_p patterns obviously consist of both zonally homogenous components (Kelvin wave-like disturbances) and localized gravity waves.

The seasonal variations described in Section 3.2 are now more clearly visible. That is, in JJA, the localized enhancement can be clearly seen from north India to southeastern Asia. In other seasons, the longitudinally elongated pattern is dominant. In particular, during DJF and MAM, the Kelvin wave-like disturbances seem to appear more dominantly than localized gravity waves, which shows a broad continuous enhancement along the longitude in the eastern hemisphere (from Africa to the western Pacific) and a separate enhancement over South America.

Zonal propagation characteristics of Kelvin waves were delineated with the CHAMP GPS RO data, assuming zonal wave number 1 and 2 (e.g., Tsai *et al*., 2004). The Kelvin wave amplitudes were enhanced around the tropopause and in the lower stratosphere between 17 and 25 km and the waves dissipated above. Ratnam *et al*. (2006a) also analyzed the long-term variations of Kelvin waves in 2001–2006 and found the largest temperature variance from the Indian Ocean to the western Pacific, with an annual cycle of wave activity with maximum wave amplitudes from November to March. The temporal and spatial distribution of E_p in Fig. 5 is consistent with these earlier results.

We now extract the latter components. From the individual panels in Fig. 2, the zonal mean of E_p is calculated at each latitude to define the longitudinally homogenous components of E_p. Then, the residual of E_p is defined as the difference from the zonal mean. The residual is again averaged for 5 years and plotted in the right panels of Fig. 5 (note the contour levels are different between the right and left panels).

In JJA, large E_p is concentrated above India, the Bay of Bengal, and the Indochina peninsula, thereby reflecting the effects of the Asian monsoon. E_p is also large over North Africa. In SON, the E_p value is relatively small in the tropics, but it is more enhanced east of the Philippines and Tibet. Note that orographic generation of mountain waves seem to be persistently active over the Andes with the largest magnitudes in SON (e.g., Hocke *et al*., 2002).

From December to May, E_p is large in the western Pacific and Indonesia. Although the E_p patterns near Indonesia may look similar between DJF and MAM, the details are different. In DJF, the centers are north-east of Papua New Guinea and between Borneo and Sumatra islands; in MAM, however, the entire pattern seems to be slightly shifted south-westward so that enhanced E_p is east of Borneo and west of Sumatra.

Alexander *et al*. (2008) analyzed the seasonal variations of gravity wave activity using tropospheric wind data collected with equatorial atmosphere radar (EAR) at Koto Ta-

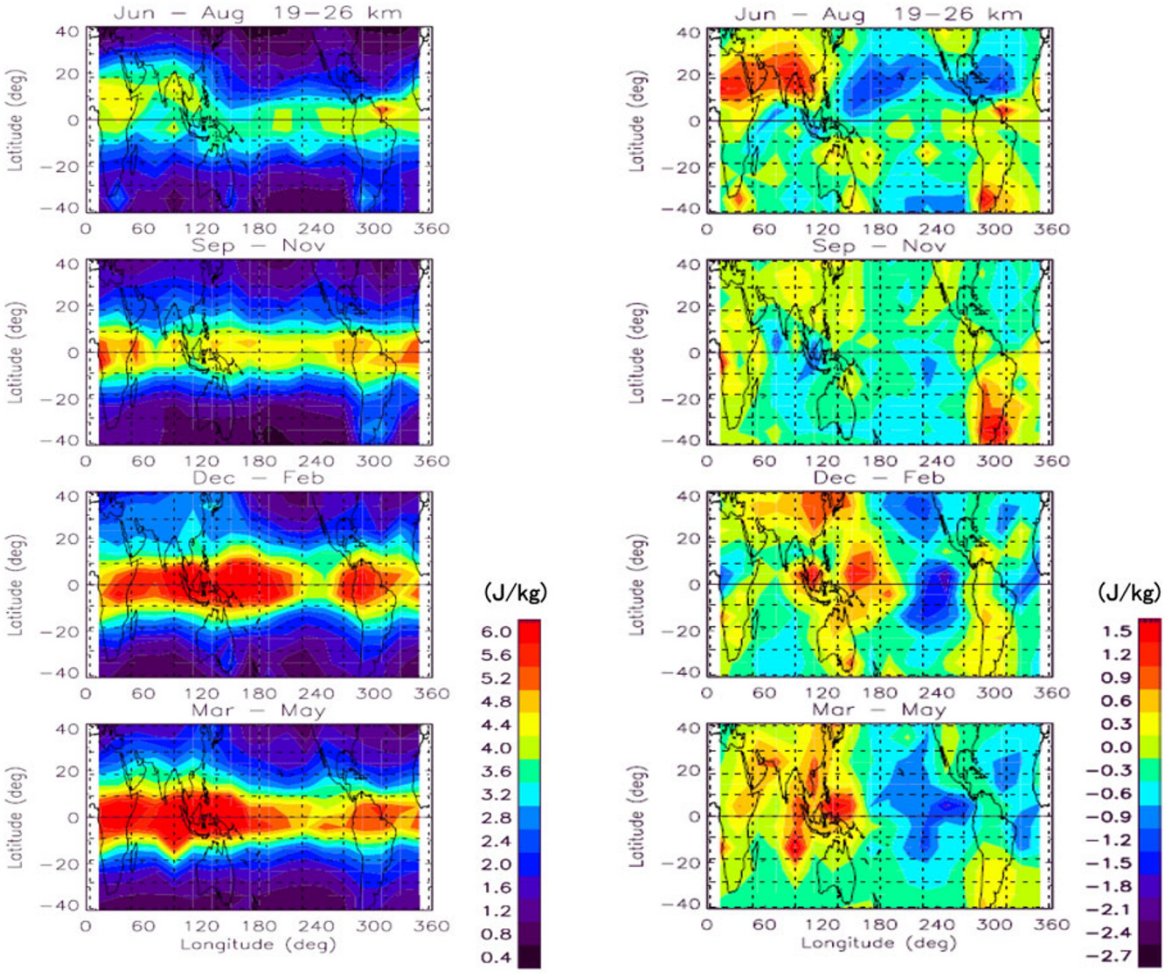

Fig. 5. Longitude-latitude distribution of E_p at 19–26 km formed by averaging the E_p results in Fig. 2 for 5 years in 2001–2006 (left). The deviation of E_p from the zonal mean is also averaged for 5 years (right). From top to bottom, the panels show the results every 3 months in June–July–August, September–October–November, December–January–February, and March–April–May, respectively.

bang, Indonesia during 2002–2006 and compared the results with OLR and TRMM-PR. They reported the primary maximum of the wind variances to be in November, with a broader secondary enhancement in March–April. They also reported that wave activity is depressed in December–January at EAR, resulting in a quasi semi-annual variation of wave activity. When these results are combined with Fig. 5, it can be suggested that the region of active gravity waves approaches the EAR site from the east and passes through toward the Indian Ocean during DJF and MAM.

Note that in the northern winter months conspicuous E_p enhancement is seen along the subtropical jet over China and Japan.

4. Concluding Remarks

Using temperature profiles observed with CHAMP GPS RO, we analyzed temperature variances with vertical scales shorter than 7 km at 19–26 km altitude and determined the gravity wave potential energy (E_p) every 3 months from June 2001 to May 2006. Temporal and spatial variations of E_p are compared with cloud parameters, i.e., OLR, and convective rain rate with TRMM-PR.

The E_p distribution in the western Pacific shows a clear seasonal variation with large enhancements in DJF and MAM. It is also large in SON. E_p is at a minimum in JJA near the equatorial western Pacific, but large E_p appears above north India, the Bay of Bengal, and the Indochina peninsula. Large E_p appears above the convective cloud regions, with the TRMM-PR results showing a better correlation than the OLR.

Kawatani *et al.* (2005) studied the horizontal distribution of gravity wave activity in the tropical stratosphere using an atmospheric general circulation model (AGCM) that assumed a July–August condition and reported a distinct longitude asymmetry in the vertical flux of the wave momentum. That is, the wave momentum flux becomes largely eastward in the eastern hemisphere, but the flux is weakly westward in the western hemisphere. Although results for only 2 months were presented, the zonal asymmetry of wave activity was also recognized throughout the year. Our results in Fig. 2 are very consistent with the prediction of this model.

Spatial distributions and seasonal variations of E_p are, in general, closely related to convective activity, but in addition to the wave generation (convection), wave propagation characteristics, such as wave-mean flow interaction with both the Walker circulation in the upper troposphere and the stratospheric QBO, must be considered in describing the

climatological behavior of E_p in the tropical stratosphere.

Acknowledgments. We deeply appreciate the valuable suggestions provided by Y. Kawatani. This study was supported in part by the Japanese Ministry of Education, Culture, Sports, Science and Technology (MEXT) through a Grant-in-Aid for Scientific Research (grant A03-13136206; A04-13136203, 13136203 and 1943009). The TRMM PR data were provided by the Japan Aerospace Exploration Agency (JAXA) and routine radiosonde data at Kuala Lumpur were provided by the Malaysian Meteorological Department. Two of the authors (V. M. R. and S. P. A.) were in receipt of a Japan Society for the Promotion of Sciences (JSPS) postdoctoral fellowship.

References

Alexander, S. P., T. Tsuda, Y. Shibagaki, and T. Koze, Seasonal Gravity Wave Activity Observed with the Equatorial Atmosphere Radar (EAR) and its relation to the Tropical Rainfall Measuring Mission (TRMM), *J. Geophys. Res.*, **113**, D02104, doi:10.1029/2007JD008777, 2008.

de la Torre, A., T. Schmidt, and J. Wickert, A global analysis of wave potential energy in the lower stratosphere derived from 5 years of GPS radio occultation data with CHAMP, *Geophys. Res. Lett.*, **33**, L248009, doi:10.10292/2006GL027696, 2006.

Fritts, D. C. and M. J. Alexander, Gravity wave dynamics and effects in the middle atmosphere, *Rev. Geophys.*, **41**, doi:10.1029/2001RG000106, 2003.

Hei, H., T. Tsuda, and T. Hirooka, Characteristics of Atmospheric Gravity Wave Activity in the Polar Regions Revealed by GPS Radio Occultation Data with CHAMP, *J. Geophys. Res.*, 2008 (in print).

Hocke, K., T. Tsuda, and A. de la Torre, A study of stratospheric gravity wave fluctuations and sporadic E at mid latitudes with focus on possible orographic effect of Andes, *J. Geophys. Res. (Atmos.)*, **107**, doi:10.1029/2001JD001330, 2002.

Holton, J. R., M. J. Alexander, and M. T. Boehm, Evidence for short vertical wavelength Kelvin waves in the Department of Energy-Atmospheric Radiation Measurement Nauru99 radiosonde data, *J. Geophys. Res.*, **106**(D17), 20,125–20,130, 2001.

Kawatani, Y., K. Tsuji, and M. Takahashi, Zonally non-uniform distribution of equatorial gravity waves in an atmospheric general circulation model, *Geophys. Res. Lett.*, **32**, L23815, doi:10.1029/2005GL024068, 2005.

Kozu, T., T. Kawanishi, H. Kuroiwa, M. Kojima, K. Oikawa, H. Kumagai, K. Okamoto, M. Okumura, H. Nakatsuka, and K. Nichikawa, Development of precipitation radar onboard the Tropical Rainfall Measuring Mission (TRMM) satellite, *IEEE Trans. Geosci. Remote Sens.*, **39**(1), 102–116, 2001.

Randel, W. J. and F. Wu, Kelvin wave variability near the equatorial tropopause observed in GPS radio occultation measurements, *J. Geophys. Res.*, **110**, doi:10.1029/2004JD005006, 2005.

Ratnam, M. V., G. Tetzlaff, and C. Jacobi, Global and Seasonal Variations of Stratospheric Gravity Wave Activity Deduced from the CHAMP/GPS Satellite, *J. Atmos. Sci.*, **61**, 1610–1620, 2004.

Ratnam, M. V., T. Tsuda, T. Kozu, and S. Mori, Long-term behavior of the Kelvin waves revealed by CHAMP/GPS RO measurements and their effects on the tropopause structure, *Ann. Geophys.*, **24**, 1355–1366, 2006a.

Ratnam, M. V., T. Tsuda, Y. Shibagaki, T. Kozu, and S. Mori, Gravity Wave Characteristics over the Equator Observed During the CPEA Campaign using Simultaneous Data from Multiple Stations, *J. Meteor. Soc. Jpn.*, **84A**, 239–257, 2006b.

Sato, K. and T. J. Dunkerton, Estimation of momentum flux associated with equatorial Kelvin and gravity waves, *J. Geophys. Res.*, **102**, 26,247–26,261, 1997.

Tsai, H.-F., T. Tsuda, Y. Aoyama, G. A. Hajj, and J. Wickert, Equatorial Kelvin Waves Observed with GPS Occultation Measurements (CHAMP and SAC-C), *J. Meteor. Soc. Jpn.*, **82**(1B), 397–406, 2004.

Tsuda, T., Y. Murayama, H. Wiryosumarto, S. W. B. Harijono, and S. Kato, Radiosonde observations of equatorial atmosphere dynamics over Indonesia, Part II: Characteristics of gravity waves, *J. Geophys. Res.*, **99**, 10507–10516, 1994.

Tsuda, T., M. Nishida, C. Rocken, and R. H. Ware, A global morphology of gravity wave activity in the stratosphere revealed by the GPS occultation data (GPS/MET), *J. Geophys. Res. (Atmos.)*, **105**, 7257–7273, 2000.

Tsuda, T., M. V. Ratnam, T. Kozu, and S. Mori, Characteristics of 10-day Kelvin Wave Observed with Radiosondes and CHAMP/GPS Occultation during the CPEA Campaign (April–May, 2004), *J. Meteor. Soc. Jpn.*, **84A**, 277–293, 2006.

Wickert, J., Ch. Reigber, G. Beyerle, R. Koig, C. Marquardt, T. Schmidt, L. Grunwaldt, R. Galas, T. Meehan, W. Melbourne, and K. Hocke, Atmospheric soundings by GPS radio occultation: First results from CHAMP, *Geophys. Res. Lett.*, **28**, 3263–3266, 2001.

T. Tsuda (e-mail: tsuda@rish.kyoto-u.ac.jp), M. Venkat Ratnam, S. P. Alexander, T. Kozu, and Y. Takayabu